THEORETICAL EVALUATION OF KOMPSAT-5 X-BAND SAR FOR OCEAN WIND RETRIEVAL

Duk-jin Kim, Younsoo Kim, and Yongseung Kim

Space Application Center, Korea Aerospace Research Institute, Daejeon, 305-333, Korea

ABSTRACT: Korean Multi-Purpose SATellite 5 (KOMPSAT-5) will be the first high resolution X-band SAR satellite of Korea. A critical parameter necessary for interpreting SAR images over the ocean is surface wind field. SAR is the only system that can provide a synoptic view of wind fields over the ocean covering large areas. However, there has been no X-band wind retrieval model. In this study, we evaluate the development of an X-band wind retrieval model and show the possibility of KOMPSAT-5 SAR on wind estimations using a combination of theoretical models.
KEY WORDS: KOMPSAT-5, wind speed, wind direction, numerical simulation

1. INTORDUCTION

KOrean Multi-Purpose SATellite 5 (KOMPSAT-5) will be the first high resolution radar satellite of Korea, which is planned for launch in 2010 (Kim and Lee, 2002). The mission was setup to produce operational remote sensing products from a space-borne X-band synthetic aperture radar (SAR) system. The SAR system can observe the Earth's surface with the very high resolution and large spatial coverage, which makes it a valuable tool for measuring geophysical parameters such as ocean surface winds, waves and currents. Although space-based scatterometers have provided global wind information for a wide range of applications, the relatively low spatial resolution of the scatterometer (25 km × 25 km) made it difficult to obtain wind information in coastal areas.

The wind information is a critical parameter to interpret SAR images over the ocean, because the dominant scattering mechanism (affecting the SAR intensity over the ocean) is Bragg scattering at moderate angles of incidence – as the wind speed increases, the height of waves at the Bragg wavelength increases (Valenzuela, 1978). The wind field extracted from the SAR measurements is valuable and can be used in many area of application such as local forecasting, typhoon monitoring, coastal engineering, energy production (wind turbine installation), ship navigation, and so on, because there is only limited information available on the ocean.

Most methods for inversion of wind vectors from SAR images use a geophysical model function (GMF) such as the CMOD series in combination with wind directions derived from wind aligned effects in the SAR image or from the external source of the wind direction to estimate wind speed (Stoffelen and Anderson, 1997; Hersbach, 2007). But the CMOD series wind GMF is only applicable to C-band VV-polarization radar data (e.g. ERS, ENVISAT and RADARSAT), and there has been no X-band GMF developed for wind estimation. In this study, we evaluate the development of the X-band wind retrieval model and the possibility of KOMPSAT-5 SAR on wind estimates using a combination of theoretical models – a radar backscattering model and a hydrodynamic interaction model.

2. NUMERICAL MODELS FOR SAR SIMULATION

2.1 Radar backscattering model

The radar backscattering model was developed for electromagnetic scattering from rough surface using the two-scale (tilted Bragg) model. The two-scale model was based on resonant Bragg scattering theory, and the normalized radar cross section (NRCS) of a slightly tilted surface of the ocean is proportional to the wave height spectral density of the Bragg waves which are in resonance with the electromagnetic waves (Wright, 1968; Lyzenga and Bennet, 1988; Romeiser et al, 1997).

The tilted Bragg contribution to the NRCS can be written as an integral over the surface slopes,

$$\sigma_B^0(\theta,\phi) = 8\pi k_0^4 \iint \left|G(\theta,\eta_x,\eta_y)\right|^2 \cdot \Psi(2k_0\sin\theta',\phi)\, p(\eta_x,\eta_y)\, d\eta_x d\eta_y \quad (1)$$

where θ is the incidence angle, ϕ is the radar look direction, k_0 is the electromagnetic wave number, η_x is the surface slope in the plane of incidence, η_y is the surface slope in the orthogonal direction, $G(\theta,\eta_x,\eta_y)$ is a polarization-dependent scattering coefficient, $\Psi(k,\phi)$ is the surface elevation spectral density, and $p(\eta_x,\eta_y)$ is the large-scale slope probability density function. Using the small-slope approximation discussed by Wright (1968), the scattering coefficients for vertical (VV) and horizontal (HH) polarization are given by

$$G_{VV}(\theta,\eta_x,\eta_y) = \frac{(\varepsilon-1)\left[\varepsilon(1+\sin^2\theta') - \sin^2\theta'\right]}{\left[\varepsilon\cos\theta + \sqrt{\varepsilon-\sin^2\theta'}\right]^2}\cos^2\theta' \quad (2)$$

$$G_{HH}(\theta,\eta_x,\eta_y) = \frac{(\varepsilon-1)\cos^2\theta'}{\left[\cos\theta + \sqrt{\varepsilon-\sin^2\theta'}\right]^2} + G_{VV}\frac{\eta_y^2}{\sin^2\theta'} \quad (3)$$

where ε is the relative dielectric constant of the ocean and $\theta' = \theta + \tan^{-1}\eta_x$ is the local incidence angle for a patch having a slope η_x in the plane of incidence.

The total NRCS is obtained by adding the physical optics or specular contribution to the tilted Bragg contribution (Barrick, 1968),

$$\sigma_s(\theta,\phi)=\frac{\pi}{\cos^4\theta}\left|R(0)\right|^2 p(\tan\theta,0) \tag{4}$$

where $R(0)=\frac{1-\varepsilon}{1+\varepsilon}$ is the Fresnel reflection coefficient for normal incidence.

2.2 Hydrodynamic interaction model

The wave height spectral density ($\Psi(k,\phi)$) is modelled by the hydrodynamic interaction model that can solve the high-wavenumber portion of the wind-wave by the action balance equation (Komen et al., 1994),

$$\frac{\partial N}{\partial t}+\left(U+C_g\right)\frac{\partial N}{\partial x}-\left(k\frac{\partial U}{\partial x}\right)\frac{\partial N}{\partial k}=S(k,x,t) \tag{5}$$

where N is the action spectral density, C_g is the group velocity, U is the surface current, and x and k is the spatial position and wave-number of the surface waves, respectively. The quantity S on the right-hand side of the equation is the net source function which accounts for wind input and wave energy dissipation (Hughes, 1978; Thompson and Gasparovic, 1986):

$$S=\mu N\left(1-\frac{N}{N_0}\right) \tag{6}$$

where μ is a wave relaxation rate and N_0 is the equilibrium action spectral density. For μ we have used the growth parameter suggested by Plant (1982),

$$\mu=0.043\left(\frac{u_*}{c}\right)^2\omega\left|\cos(\phi-\phi_w)\right| \tag{7}$$

where u_* denotes the friction velocity, $c=\omega/k$ is the phase velocity, and ϕ_w is the wind direction. The relationship between the action spectral density (N) and the wave height spectrum (Ψ) is given by (Phillips, 1977)

$$N(k,\phi)=\rho\frac{\omega}{k}\Psi(k,\phi) \tag{8}$$

where ω is the intrinsic wave frequency, which is given by

$$\omega=\sqrt{gk+\frac{\tau}{\rho}k^3} \tag{9}$$

where g is the gravitational acceleration, τ is the surface tension, and ρ is the density of water.

To solve the action spectral density, N, as a function of the four coordinates x, y, k, ϕ, the two spatial coordinates, x and y are assumed to lie on a regular Cartesian grid, the wave direction, ϕ, is distributed evenly over the interval $(0, 2\pi)$. However, a logarithmic grid is used for the wave-number, k, since the solution is required over many orders of magnitude of this coordinate.

3. NUMERICAL SIMULATION RESULTS

The ocean wave equilibrium spectrum is required to calculate the NRCS of ocean surface using the two-scale radar backscattering model and the hydrodynamic interaction model. Since the short waves are intimately coupled with intermediate and long-scale waves, we need a full wave-number model. In this study, among the wave spectrum models that are widely used in microwave radar scattering studies, we used Romeiser's (1997) ocean wave spectrum because it is optimized using a variety of NRCS values measured from airborne scatterometers for different wind speeds, polarizations, incidence angles, and radar frequencies including X-band measurements (Figure 1).

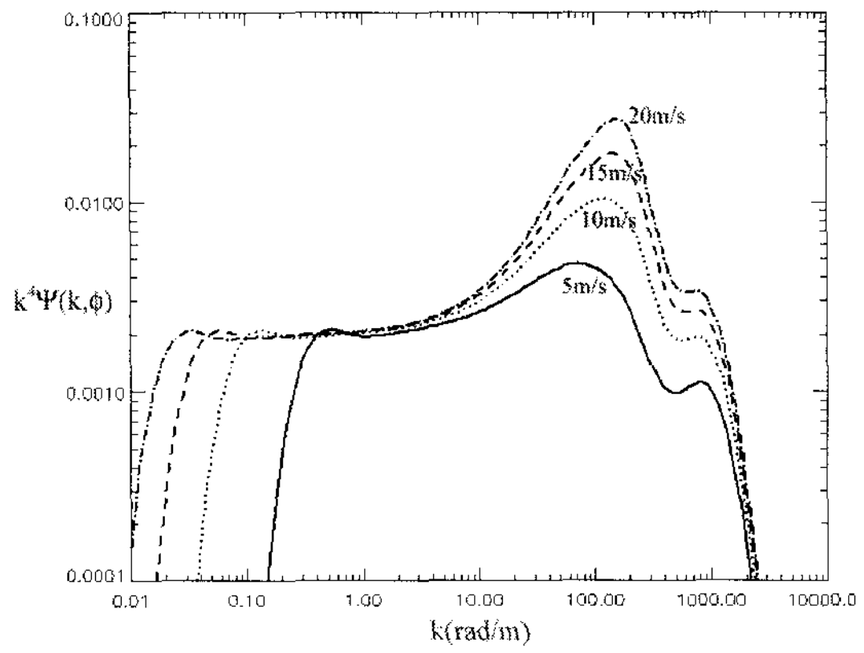

Figure 1. Romeiser's (curvature) ocean wave spectrum at $\phi=0$ for four wind speeds.

In order to test the performance of the numerical model simulation, we have compared the NRCSs calculated from the radar backscattering model and the hydrodynamic interaction model with the CMOD4 model function (Figure 2). The CMOD4 model function was derived empirically using a large number of C-band, VV-polarization NRCS measurements made by the ERS-1 scatterometer over an incidence angle range from 18° to 57° and a wind speed range from about 0-20 m/s (Stoffelen and Anderson, 1997). For NRCS calculations, numerical simulations were made at C-band (5.3 GHz) VV-polarization for incidence angles from 20° to 60°, wind speed values ranging from 2 to 30 m/s and wind direction ranging from 0 to 360°. Although the NRCSs simulated from numerical models are somewhat higher than the results of CMOD4 model function, they are linearly related. It represents that the radar backscattering

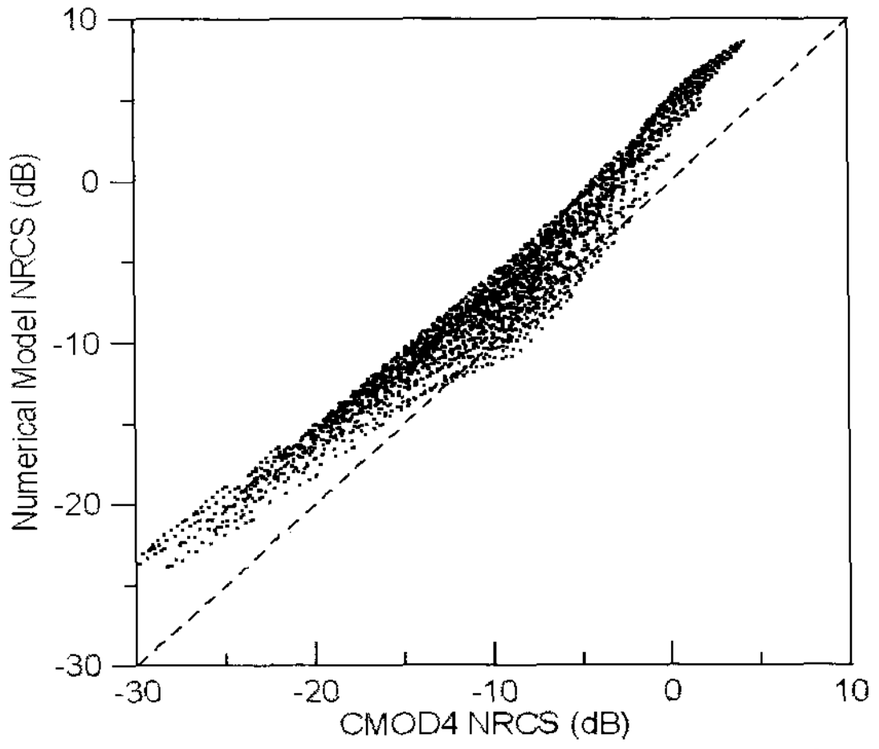

Figure 2. Relationship between NRCSs from CMOD4 model function and from the numerical model simulation.

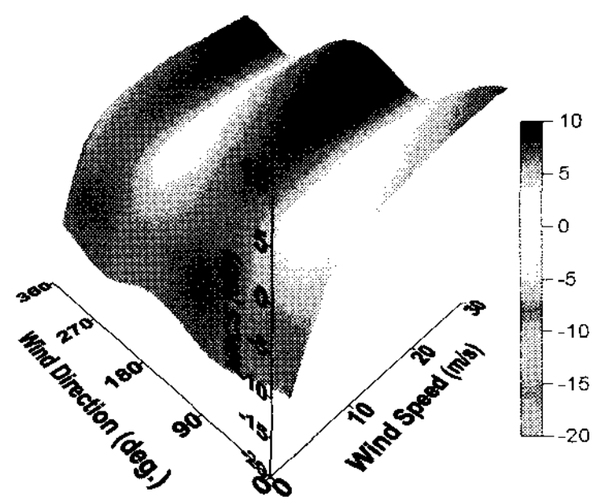

(a)

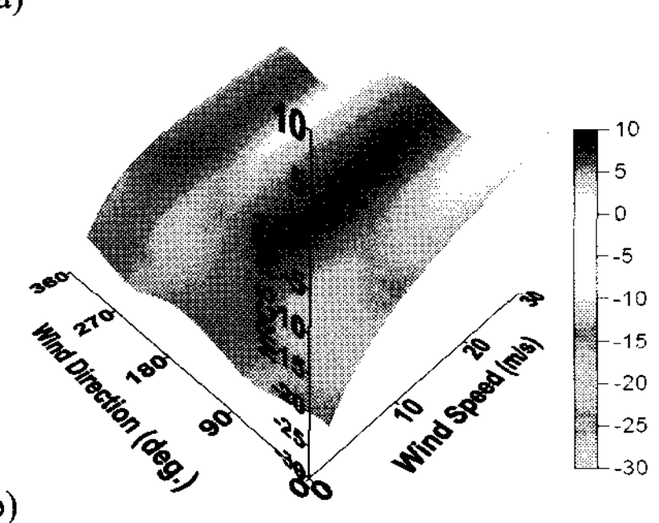

(b)

Figure 3. Simulated X-band NRCS as a function of wind speed and wind direction for VV-polarization. (a) incidence angle of 25°; (b) incidence angle of 45°.

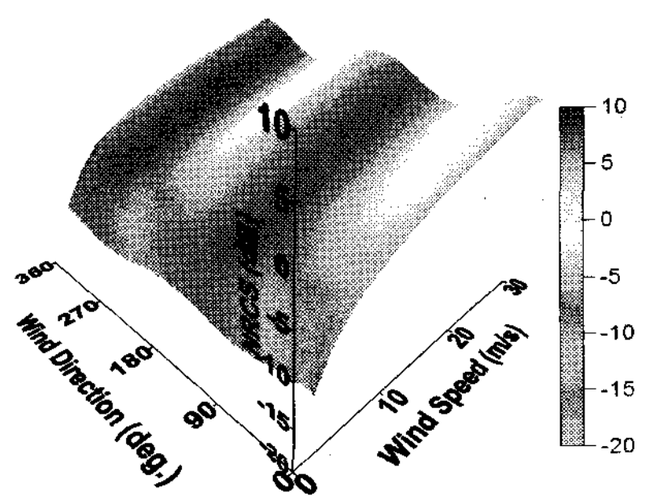

(a)

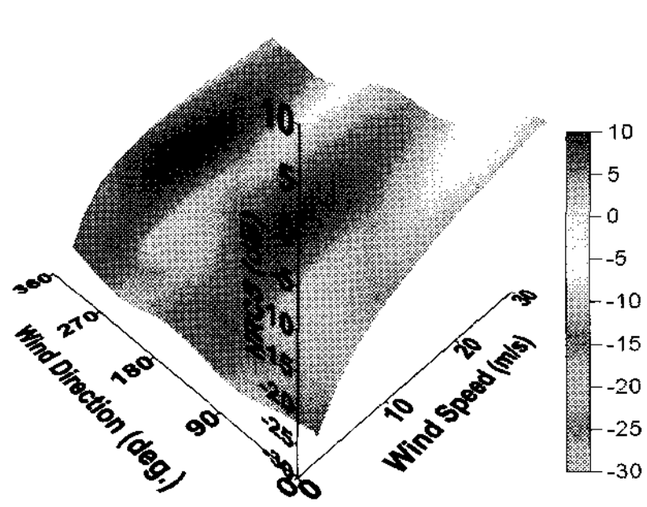

(b)

Figure 4. CMOD4 NRCS as a function of wind speed and wind direction for VV-polarization. (a) incidence angle of 25°; (b) incidence angle of 45°.

model and hydrodynamic interaction model reasonably well predict the values of NRCS at given incidence angles, wind speed, and wind direction ranges. Furthermore the relative accuracy of the predicted NRCS is much better than the absolute.

Using the performance ability of the numerical models, we have also simulated the NRCSs at X-band (9.65 GHz) for both vertical and horizontal polarization for the same ranges of incidence angle, wind speed, and wind direction as in Figure 2. The simulated data of X-band showed the explicit dependence of wind speed and wind direction (Figure 3) as the CMOD4 model function does (Figure 4). Note that the NRCS of X-band is higher than the NRCS of CMOD4 at given wind speed and direction, and the sensitivity of X-band NRCS on wind speed is higher at low wind speeds. This is because a higher radar frequency is more sensitive to shorter ocean surface waves, resulting in more sensitivity to wind variation at low winds. Figure 5 shows the simulated X-band NRCS as a function of wind direction. One can observe the sinusoidal behaviour of the NRCS as a function of wind direction.

We also investigated the radiometric resolution and the noise equivalent σ° required for developing X-band wind retrieval model. Since it is generally accepted that a typical accuracy of wind speed is ±2 m/s, we plotted the ΔNRCS of 2 m/s intervals as function of wind speed (Figure 6). The mean value of ΔNRCS was 1.37 dB, but the radiometric resolution of 0.5 dB is recommended for the required accuracy over a broad range of wind speeds.

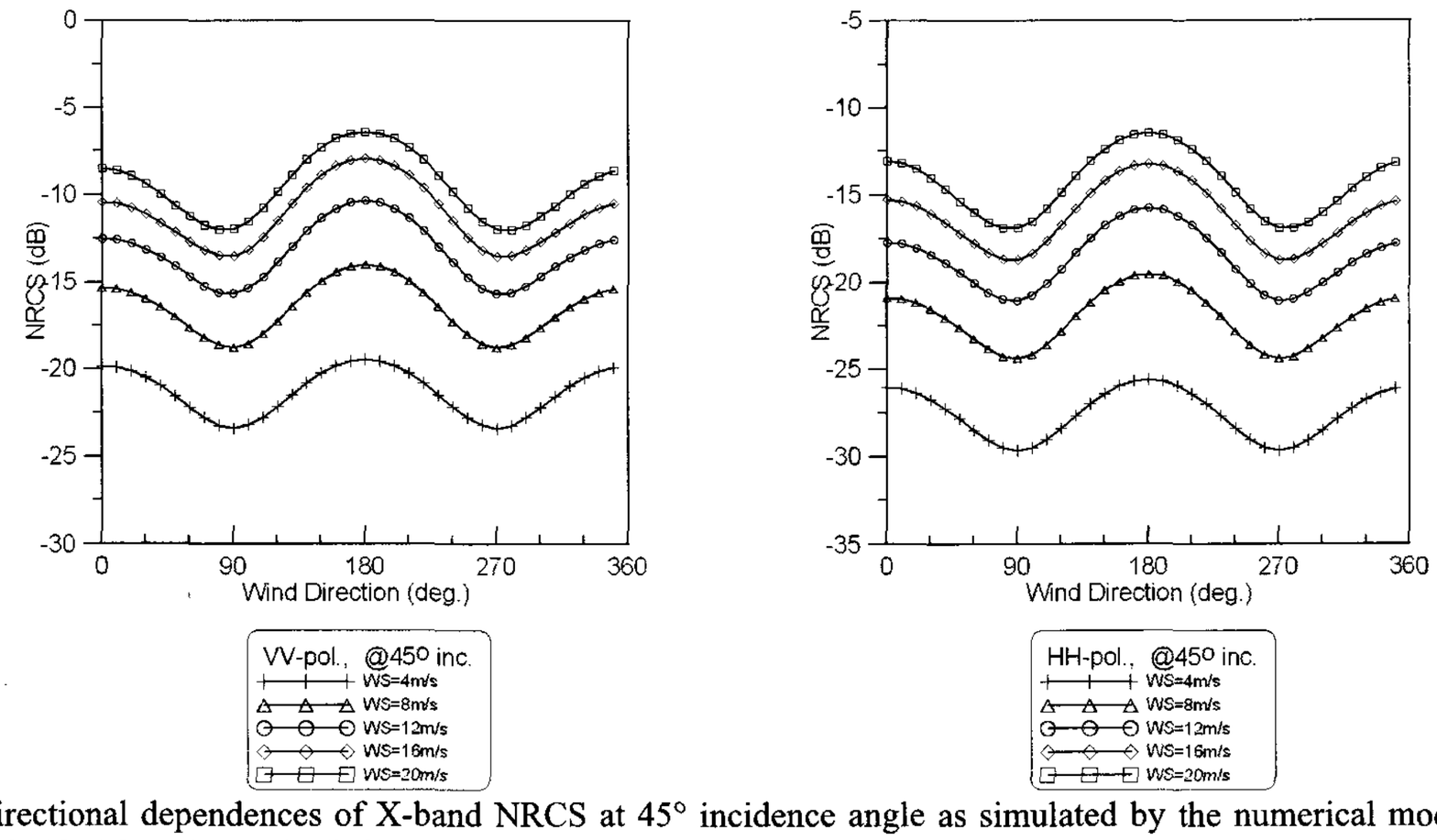

Figure 5. Directional dependences of X-band NRCS at 45° incidence angle as simulated by the numerical models for wind speeds of 4, 8, 12, 16, and 20 m/s. (left) VV-polarization; (right) HH-polarization.

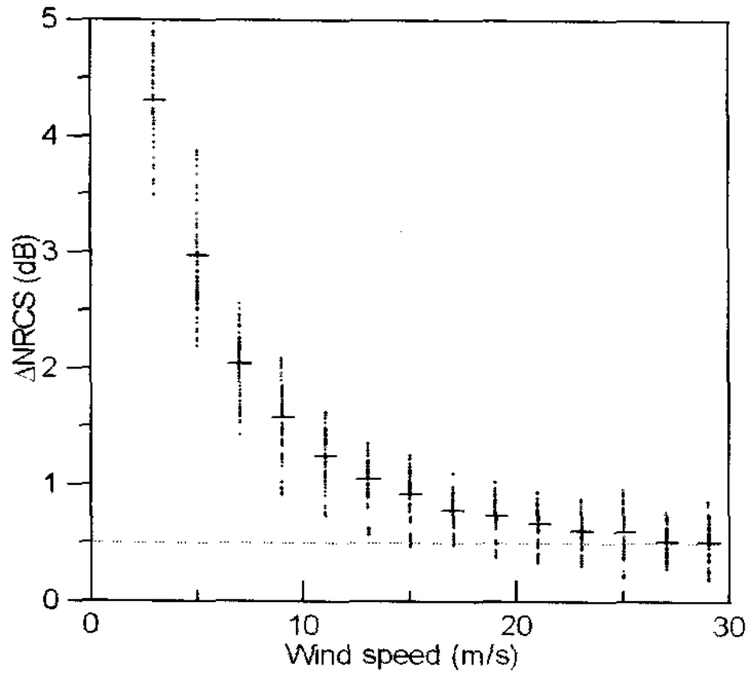

Figure 6. ΔNRCS as function of wind speed. The ΔNRCS was calculated by subtracting the NRCSs of 2 m/s wind intervals.

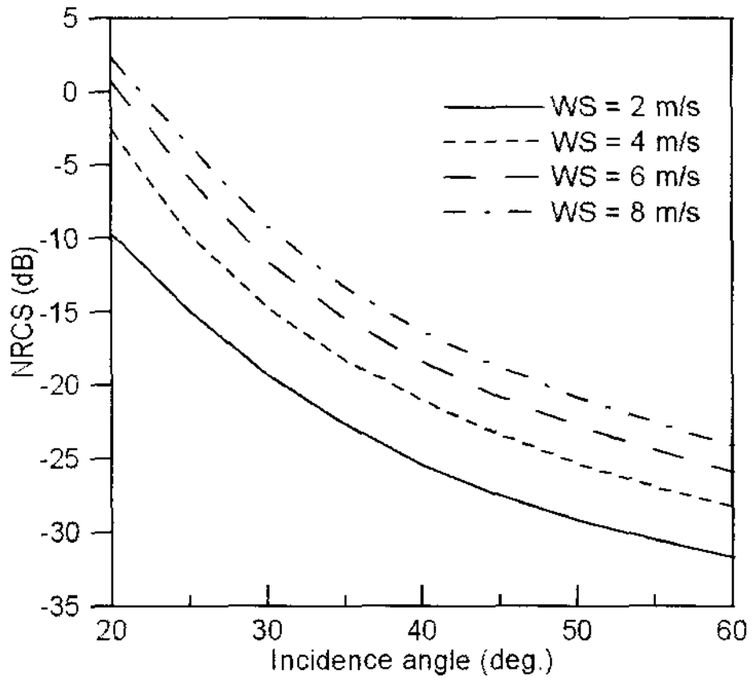

Figure 7. The minimum NRCS as function of incidence angle for VV-polarization.

Noise equivalent σ° is a fundamental parameter in any SAR application. In wind retrieval application, the noise equivalent σ° defines the minimum detectable wind speed. Figure 7 shows the minimum NRCS (cross-wind case, i.e., relative wind direction of 90° or 270°) as function of incidence angle for VV-polarization and for wind speeds of 2, 4, 6, and 8 m/s. For example, if one would like to detect low wind speed of 2 m/s, the noise equivalent σ° should be below -30 dB at high incidence angle ranges.

4. DISCUSSION AND CONCLUSION

The state of the ocean surface depends on the wind speed and direction, as well as a number of other parameters such as the fetch and duration of the wind, the air-sea temperature difference, the current gradients, and the presence of surfactant materials. If the wind speed is constant for a sufficiently long time and the fetch is sufficiently large, the ocean surface is believed to approach an equilibrium state. However, in real situations, this does not always happen. Therefore, our evaluation for X-band wind retrieval based on the numerical simulation may not be accurate. Since the results of numerical simulation, despite such limitation, showed the explicit dependence of wind speed and direction, and since the polarization and incidence angle dependences of NRCS were also consistent with the typical observations from the ocean, it would be possible to develop X-band GMF for wind estimates.

REFERENCES

Barrick, D.E., 1968, Rough surface scattering based on the specular point theory, *IEEE Trans. Antennas Propag.*, AP-16, pp. 449-454.

Hersbach, H., A. Stoffelen, and S. de Hann, 2007, An improved C-band scatterometer ocean geophysical model function: CMOD5, *J. Geophys. Res.*, 112(C03006), doi:10.1029/2006JC003743.

Hughes, B.A., 1978, The effect of internal waves on surface wind waves, 2. Theoretical analysis, *J. Geophys. Res.*, 83, pp. 455-465.

Kim, Y.-S. and S.-R. Lee, 2002, Feasibility study of synthetic aperture radar – Adaptability of the payload to KOMPSAT platform, *J. Astron. Space Sci.*, 19(3), pp. 225-230.

Komen, G.J., Cavaleri, L., Donelan, M., Hasselmann, K., Hasselmann, S. and P.A.E.M. Janssen, 1994: *Dynamics and Modelling of Ocean Waves*, Cambridge University Press, 532 p.

Lyzenga, D.R. and J.R. Bennett, 1988, Full-spectrum modeling of synthetic aperture radar internal wave signatures, *J. Geophys. Res.*, 93(c10), pp. 12345-12354.

Phillips, O.M., 1977, *The Dynamics of the Upper Ocean*, 2nd ed., 336 pp., Cambridge University Press, New York.

Plant, W.J., 1982, A relationship between wind stress and wave slope, *J. Geophys. Res.*, 87, pp. 1961-1967.

Romeiser, R., W. Alpers, and V. Wismann, 1997, An improved composite surface model for the radar backscattering cross section of the ocean surface 1. Theory of the model and optimization/validation by scatterometer data, *J. Geophys. Res.*, 102(C11), 25237-25250.

Stoffelen, A. and D. Anderson, 1997, Scatterometer data interpretation: Estimation and validation of the transfer function CMOD4, *J. Geophys. Res.*, 102, pp. 5767-5780.

Thompson, D.R., and R.F. Gasparovic, 1986, Intensity modulation in SAR images of internal waves, *Nature*, 320, pp. 345-348.

Valenzuela, G. R., 1978, Theories for the Interaction of Electromagnetic and Ocean Waves – A Review, *Boundary Layer Meteorology,* 13, pp. 61-85.

Wright, J.W., 1968, A new model of sea clutter, *IEEE Trans. Antennas Propag.*, AP-16, pp. 217-223.